E-ISSN: 111 – 2716 P-ISSN: 3026 – 8214
MPRI-JAAER | INTERNATIONAL JOURNAL OF APPLIED & ADVANCED ENGINEERING RES.
VOL. 14 NO. 5 OCTOBER, 2026

ESTIMATING ORIGINAL OIL IN PLACE IN A NIGER DELTA BLACK-OIL RESERVOIR: CONSTRAINING MATERIAL BALANCE NON-UNIQUENESS VIA PVT COUPLING AND ENERGY-BUDGET SCREENING

EMMANUEL DOYAH[1]; DANIEL UCHECHUKWU IBOBO[1]; OKPERHIE JOHNBULL[1]; PERCY OJOGBO[1]; EMMANUEL TEGA EROKARE[2]; & WISDOM CHUKWUEMEKE ULAKPA[3]

[1]Department of Petroleum Engineering, Faculty of Engineering, Southern Delta University, Ozoro, Nigeria. [2]Department of Agricultural and Biosystems, Engineering, Faculty of Engineering, Southern Delta University, Ozoro, Nigeria. [3]Department of Chemical Engineering, Faculty of Engineering, Southern Delta University, Ozoro, Nigeria
Corresponding Author: ulakpa.wisdom@yahoo.com
DOI: https://doi.org/10.70382/mejaaer.v14i5.068

Abstract

This study estimates the original oil in place (OOIP) of a Niger Delta black-oil reservoir by integrating PVT characterisation in PVTp with single-tank material balance in MBAL (Petroleum Experts IPM suite), and by validating the result against an independent Havlena–Odeh energy-budget calculation. A ten-year production and pressure history (October 2008–September 2018; 60.51 MMSTB produced; pressure declined from 2,671.7 to 1,726.7 psia) was matched using a black-oil description anchored to laboratory saturation data (P_b ≈ 2,643.76 psia; R_{si} = 566 scf/STB; B_{oi} = 1.3358 RB/STB; μ_o = 0.579 cp). Six PVT correlations were regressed with multiplier–shift modifiers: Standing gave the best bubble-point match ($\sigma = 2.44 \times 10^{-8}$), while Vasquez–Beggs performed best for solution GOR (σ = 2.726) and oil FVF (σ = 0.00283), with modifiers close to unity. Two radial aquifer models were evaluated: a Carter–Tracy 360° case returned 500 MMSTB (RF ≈ 12.1%), whereas a Hurst–van Everdingen–Dake 180° case, supported by a sensitivity minimum between roughly 120° and 200° encroachment angle,

Keywords: Original Oil in Place (OOIP); Material Balance; Water Influx; Havlena–Odeh; Niger Delta; Black-Oil PVT.

EDITOR-IN-CHIEF
Prof. Saeid Eslamian [IRAN]

returned 310 MMSTB (RF ≈ 19.5%) — a 38% spread constituting the dominant uncertainty. The energy plot attributes 55–60% of the drive to fluid expansion, 40–45% to water influx and about 2% to pore-volume compressibility; there is no gas cap. A separate energy budget gives an underground withdrawal of 106.5 MMRB at R_p = 700 scf/STB (101.9–111.1 MMRB for R_p between 650 and 750 scf/STB). At N = 310 MMSTB this leaves an implied water influx of approximately 36 MMRB (32–41 MMRB). At N = 500 MMSTB the expansion terms alone (≈113 MMRB) exceed the withdrawal, so the implied influx would have to be negative, which is physically inadmissible. The budget therefore caps OOIP at approximately 450–490 MMSTB: the 500 MMSTB result falls outside that limit and the 310 MMSTB result sits comfortably within it. The fluid description adds only a modest, well-bounded uncertainty, the aquifer description dominates, and a first-order energy budget can rule out inadmissible aquifer models before expensive volumetric or simulation work begins.

Introduction

Any estimate of original oil in place (OOIP) is thus an estimate of a volume never measured directly by a well. Reservoir engineering has always involved indirect inference from the observed response of pressure, production rates, and fluid properties. It is the earliest and least expensive of the inferences. It balances the voidage created by production with expansion of octane, dissolved gas, connate water and rock, and influx of water from the aquifer. It remains useful in the field because it does not require detailed input data (cost) other than average reservoir pressure, cumulative production, and normal fluid properties and is applied to homogeneous, fractured, and unconventional systems (Fuentes-Cruz et al., 2021; Li et al., 2024; Tian et al., 2025).

Recent applications have adapted the approach for complex systems with aquifer support. The injunction that the method is only as good as its input's reigns for two of them. One is the fluid characterisation. The expansion terms are given by the formation volume factors and solution gas-oil ratio, defined in the laboratory if a representative sample is available, otherwise they are calculated from correlations (which are known to be sensitive to the location and crude the correlations are derived from) (Li al., 2025; Jongkittinarukorn et al., 2023). Explicit quality-control procedures based on mass-balance have also highlighted the need to establish the credibility of laboratory PVT before it is used in material-balance calculations (Papanikolaou et al., 2024). For bubble-point pressure and formation volume factor, correlations and machine-learning models developed locally for Niger Delta crudes have consistently performed better than imported ones (Obanijesu et al., 2008; Ikpabi andAkinsete, 2022), suggesting that the choice of correlation is itself a modelling decision with downstream consequences.

Second input is the aquifer. The problem is that the material balance equation is a single equation and there are many unknowns (i.e., oil in place, gas cap size, and water influx) therefore there can be many combinations that reproduce the same pressure history and a good fit is not a necessary

EDITOR-IN-CHIEF
Prof. Saeid Eslamian [IRAN]

condition for properly characterising the reservoir-aquifer system (Fuentes-Cruz et al. 2021). New material-balance formulations that simultaneously estimate the in-place volumes and aquifer parameters continue to address this nonuniqueness (Jongkittinarukorn et al., 2023; Li et al., 2025). Commercial material-balance codes have made both inputs adjustable and abusable. Evidence of this comes from studies looking at the Petroleum Experts MBAL module: aquifer model choice affected fitted size and quality of regression in one case and the matching from the Fetkovich model adjustments ended up being made in a Niger Delta study only after regression of the fluid and rock properties in that (Nmegbu et al., 2021; Saleh et al., 2025). Water drive studies elsewhere demonstrate the same sensitivity, with the oil in place and the extent of aquifer support depending on the choice of influx model (Al-Mahasneh et al., 2023; Aliu et al., 2024). What is typically not done in these studies is to carry a single fluid model from characterisation to material balance, quantify the contribution of each stage to the final uncertainty, and then test the answer with an independent calculation that does not rely on the software regression.

The novelty here is that a single fluid description (tied to PVT characterisation, no re-entry) is carried from PVT characterisation to material balance, locking all OOIP results for the case study down into a single fluid mode, and then closing the loop with an early Havlena–Odeh energy-budget check independent of the software's regression. Most material-balance case studies report (but do not test) a history match; this work (i) gives a common means of quantitatively assessing the uncertainty contributed by each stage (fluid correlations vs. aquifer description) and so can rank them, and (ii) displaces the qualitative way of seeing non-uniqueness of material balance by a quantitative, arithmetic screen that tells the engineer first, when is the aquifer model impossible, and what are the impossible class (360° Carter-Tracy, 500 MMSTB) aquifer models compared to a physically plausible description (180° horizontal vertical drain, 310 MMSTB)?

The paper fills that knowledge gap for Reservoir XYZ through four interconnected objectives:

1. Describe the uncertainty in each phase. 1. Stage-wise uncertainty quantification. Demonstrate that the fluid description, when correlated to laboratory data, has small, well-bounded uncertainty (correlation modifiers between 1.0; ~2 % effect on Eo on FVF choice, ~±4 % on F on bracketing of Rp), but aquifer description has largest single uncertainty: 38 % (190 MMSTB) nodding between two aquifer scenarios investigated.

2. A separate energy-budget filter. Use fluid properties same, production total (no other data), and still describe a first-order Havlena-Odeh energy budget combining the best OOIP estimate (~450-490 MMSTB, upper bound) to reduce OOIP and distinguish between aquifer-weakness models to the competitive advantage.

3. Verification by regional correlations. Show for this Niger Delta crude that the best correlation is property-dependent (Standing for Pb, Vasquez-Beggs for Rs and Bo, Lasater weakest for all three) and that regression-tuned global correlations can serve as adequate substitutes for regional models if the latter are absent.

4. Consistency and practical implications. Fluid-model inconsistency (tables computed by Glaso/Beggs-Robinson but best-rated by Standing/Vasquez-Beggs), suggest to regenerate tables from the best-rated correlations, and break down the increase of 28% of viscosity and decrease of 7% of FVF into end increases of deliverability and Vogel-type inflow behaviour. The discontinuous, bracketing jumps in pressure (220 and 132 psi) mitigate against the aquifer interpretation as

EDITOR-IN-CHIEF
Prof. Saeid Eslamian [IRAN]

discreetly possible physical explanations (gauge recal.) or incomplete shut-in or local compartmentalisation and the under-need of surveillance.

Materials and Methods

Reservoir, Data and Software

Reservoir XYZ is an oil-bearing sand in the Niger Delta, near Ozoro, modelled as a single tank at a reservoir temperature of 195 °F. The data comprised the fluid inputs required by a black-oil model, laboratory match data at the saturation pressure, a monthly production and pressure history beginning on 31 October 2008 and running to 30 September 2018 and the tank, rock and aquifer parameters of Table 1. No water or gas was injected. The analysis used three tools: Microsoft Excel for data organisation and quality control, PVTp for fluid characterisation and MBAL for material balance, the last two being modules of the Integrated Production Modelling (IPM) suite of Petroleum Experts (2018). The suite was chosen because a fluid model matched once in PVTp is carried into the tank model without re-entry, keeping the fluid description consistent between modules, and the same table can subsequently be used in the well performance module, PROSPER.

Table 1: Fluid, Tank and Aquifer Inputs used in the Study

Parameter	Value	Note
Reservoir temperature	195 °F	Constant
Produced gas–oil ratio	700 scf/STB	Black-oil input
Stock-tank oil gravity	35 °API	
Gas gravity (air = 1)	0.8	
Water salinity	10,000 ppm	
H_2S, CO_2, N_2	0 mol %	Sweet, non-hydrocarbon free
Initial reservoir pressure	2,671.7 psia	31 October 2008
Porosity	0.26	Tank
Connate water saturation	0.24	
Formation compressibility	3.233×10^{-6} psi^{-1}	
Initial gas cap	None	$m = 0$
Thickness / radius (initial model)	138 ft / 5,000 ft	Carter–Tracy case

Analytical Workflow

The workflow in Fig. 1 is sequential: the fluid model is matched and accepted before the tank model is built, ensuring that every material balance result is traceable to a single fluid description. The tank model was then regressed against the pressure history with the aquifer parameters as the principal unknowns; the regression was repeated for a second aquifer configuration, and the two resulting values of oil in place were compared. The final step, added in this study, is an independent energy-budget check that does not use the software's regression.

EDITOR-IN-CHIEF
Prof. Saeid Eslamian [IRAN]

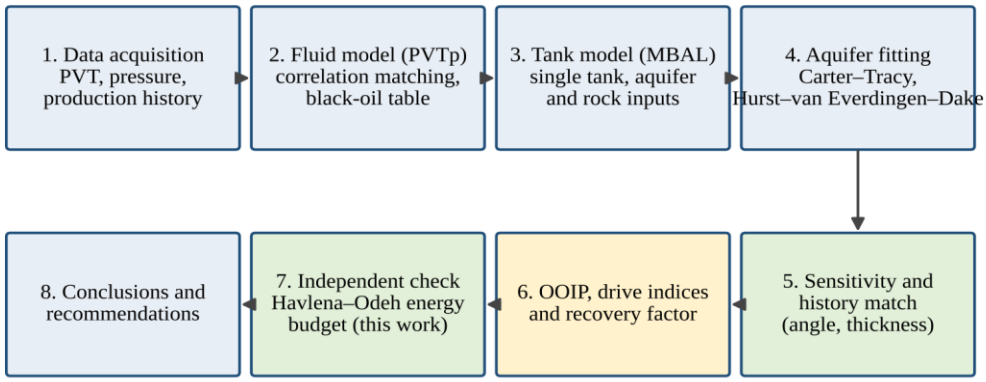

Figure 1. Analytical workflow of the study. Steps 1–6 follow the IPM suite sequence; step 7 is an independent calculation added in this work

Fluid Characterisation and Correlation Matching

The fluid was defined as a black oil because a stock-tank gravity of 35 °API and a produced gas–oil ratio of 700 scf/STB lie well below the volatile-oil range. Suitable correlations for bubble-point pressure, solution gas–oil ratio, oil formation volume factor and oil viscosity were selected for the property tables (Fotias et al., 2022). Laboratory match data at 195 °F were then entered, comprising a saturation pressure, a solution gas–oil ratio of approximately 566 scf/STB, an oil formation volume factor of 1.3358 RB/STB and a viscosity of 0.579 cp at the bubble point. Six widely used correlations were compared against these data, and recent comparative studies confirm that the relative performance of classical correlations such as Standing, Vasquez–Beggs, Glaso and Al-Marhoun remains strongly dependent on the regional fluid characteristics (Alatefi & Almeshal, 2021; Fotias et al., 2022). For illustration, the Standing correlation for bubble-point pressure and the Vasquez–Beggs correlation for solution gas–oil ratio take the forms of Eqs. 1 and 2, in which γg is gas gravity, γAPI is stock-tank gravity, T is temperature in °F, p is pressure and C1, C2 and C3 are coefficients that depend on whether the gravity is above or below 30 °API.

$$P_b = 18.2\left[\left(\frac{R_s}{\gamma_g}\right)^{0.83} 10^{0.00091\,T - 0.0125\,\gamma_{API}} - 1.4\right] \tag{1}$$

$$R_s = C_1\,\gamma_{gs}\,p^{\,C_2}\exp\left[\frac{C_3\,\gamma_{API}}{T+460}\right] \tag{2}$$

Each correlation was regressed against the laboratory data with a multiplier (a_1) and a shift (a_2) applied to the calculated property, as in Eq. 3, and the correlations were ranked by the standard deviation σ of the residuals. Modifiers close to $a_1 = 1$ and $a_2 = 0$ indicate that the unmodified correlation already describes the fluid and that the match involves little distortion.

$$y_{matched} = a_1\,y_{corr} + a_2, \qquad \sigma = \sqrt{\frac{1}{n}\sum_{i=1}^{n}\left(y_{lab,\,i} - y_{matched,\,i}\right)^2} \tag{3}$$

EDITOR-IN-CHIEF
Prof. Saeid Eslamian [IRAN]

Material Balance Formulation

For a single-tank oil reservoir with no injection, the underground withdrawal F is given by Eq. 4, in which N_p is cumulative oil, R_p the cumulative produced gas–oil ratio, R_s the solution gas–oil ratio and B_o, B_g and B_w the formation volume factors of oil, gas and water. The expansion of the oil with its dissolved gas, E_o, and of the connate water and rock, $E_{f,w}$, are defined in Eq. 5, where c_w and c_f are the water and formation compressibilities, S_{wc} is connate water saturation and Δp is the pressure drop from the initial value. With no gas cap, the material balance equation is Eq. 6, which Al-Mahasneh et al. (2023) rearranged into a straight line: a plot of $F/(E_o + E_{f,w})$ against $W_e/(E_o + E_{f,w})$ has unit slope when the aquifer is correctly modelled, and its intercept is the oil in place N.

$$F = N_p[B_o + (R_p - R_s)B_g] + W_p B_w \tag{4}$$

$$E_o = (B_o - B_{oi}) + (R_{si} - R_s)B_g, \qquad E_{f,w} = B_{oi}\,\frac{c_w S_{wc} + c_f}{1 - S_{wc}}\,\Delta p \tag{5}$$

$$F = N(E_o + E_{f,w}) + W_e \quad \Longrightarrow \quad \frac{F}{E_o + E_{f,w}} = N + \frac{W_e}{E_o + E_{f,w}} \tag{6}$$

The relative contribution of each energy source is quantified by the drive indices defined in Eq. 7, which sum to unity. In this formulation, DDI, EDI and WDI represent the depletion-drive, expansion (rock-and-water) and water-drive indices, respectively.

$$DDI + EDI + WDI = 1, \quad DDI = \frac{NE_o}{F}, \quad EDI = \frac{NE_{f,w}}{F}, \quad WDI = \frac{W_e - W_p B_w}{F} \tag{7}$$

Aquifer Models

Two radial aquifer models were applied. The Hurst–van Everdingen–Dake formulation evaluates cumulative water influx by superposing the reservoir pressure history onto a dimensionless influence function (Eq. 8), where B is the aquifer constant, RB/psi, ϑ the encroachment angle, r_e the aquifer radius, c_t the total compressibility and Q_D the dimensionless influx (Yao et al., 2024). The Carter–Tracy approximation avoids explicit superposition by employing a recursive solution (Eq. 9) expressed in terms of the dimensionless pressure P_D and its derivative. In MBAL, the dimensionless pressure is fitted with the polynomial of Eq. 10 whose coefficients a_0 to a_3 are returned by the regression together with a standard deviation of fit (Yao et al., 2024, Li et al., 2025).

$$W_e = B\sum_j \Delta p_j\, Q_D(t_D - t_{Dj}), \quad B = 1.119\,\phi\, c_t\, r_e^2\, h\,\frac{\theta}{360}, \quad t_D = \frac{0.00633\,k\,t}{\phi\,\mu_w\,c_t\,r_e^2} \tag{8}$$

$$W_{e,n} = W_{e,n-1} + (t_{Dn} - t_{D,n-1})\frac{B\,\Delta p_n - W_{e,n-1}\,P_D'(t_{Dn})}{P_D(t_{Dn}) - t_{D,n-1}\,P_D'(t_{Dn})} \tag{9}$$

$$P_D(t_D) \approx a_0 + a_1 t_D + a_2 \ln t_D + a_3 (\ln t_D)^2 \tag{10}$$

Aquifer Configurations and Sensitivity Analysis

The initial configuration was a Carter–Tracy radial aquifer with a thickness of 138 ft, a radius of 5,000 ft, an outer-to-inner radius ratio of 15, full 360° encroachment and a permeability of 700 md.

EDITOR-IN-CHIEF
Prof. Saeid Eslamian [IRAN]

A two-parameter sensitivity analysis was then run-on encroachment angle (0–400°) against thickness (100–200 ft), and the standard deviation of the regression was used as the objective. The configuration finally adopted was a Hurst–van Everdingen–Dake aquifer with a 180° angle, a radius ratio of 10, a permeability of 1,000 md and a calculated aquifer volume of 294,764 MMft^3. The relative permeability tables were supplied with no hysteresis and with water and gas sweep efficiencies of 100%.

Independent Energy-Budget Check

The regression in MBAL returns the oil-in-place as an output of the fit and does not, by itself, indicate whether a candidate value is energetically admissible. To provide such a test, the terms of Eqs. 4–6 was evaluated at the end of the history from the reported fluid properties. The solution gas–oil ratio and oil formation volume factor at 1,754.7 psia (the final pressure of 1,740 psig) were linearly extrapolated from the reported PVTp table over the range 1,814.7 to 2,689.5 psia. The gas formation volume factor was calculated using the real-gas law with Z = 0.81 (Eq. 11). The initial values were taken as B_{oi} = 1.3358 RB/STB and R_{si} = 566 scf/STB, and the cumulative oil was 60.51 MMSTB. The cumulative produced gas–oil ratio after 2009 is not reported, so R_p was bracketed at 650, 700 and 750 scf/STB around the produced gas–oil ratio of 700 scf/STB used as the fluid input. The water influx required to balance any assumed oil-in-place is given by Eq. 12, and setting it to zero yields the maximum oil-in-place, N_{max}, that the energy balance can accommodate. This is a first-order screening calculation, not a replacement for the regression: it uses end-of-history values, ignores the pressure path, and inherits the uncertainty of the extrapolation and of R_p, which is why the bracket is reported.

$$RF = \frac{N_p}{N}, \qquad B_g = 0.02829\,\frac{ZT}{p}\ \ (\mathrm{ft^3/scf}) \tag{11}$$

$$N_{max} = \frac{F}{E_o + E_{f,w}}\quad (W_e \geq 0), \qquad \hat{W}_e(N) = F - N(E_o + E_{f,w}) \tag{12}$$

The inputs and intermediate values of the calculation are listed in Table 2 so that it can be reproduced.

Table 2. Inputs and Intermediate Values of the Energy-Budget Check (R_p = 700 scf/STB, p = 1,754.7 psia).

Quantity	Value	Source
Cumulative oil, N_p	60.51 MMSTB	MBAL history
Oil FVF, B_o (extrapolated)	1.2374 RB/STB	PVTp table, linear
Solution GOR, R_s (extrapolated)	357.1 scf/STB	PVTp table, linear
Gas FVF, B_g	0.001523 RB/scf	Eq. 11, Z = 0.81, T = 654.7 °R
Initial FVF and GOR, B_{oi}, R_{si}	1.3358 RB/STB, 566 scf/STB	Laboratory match data
Oil expansion, E_o	0.2197 RB/STB	Eq. 5
Rock and water expansion, $E_{f,w}$	0.0064 RB/STB	Eq. 5, Δp = 917 psi
Withdrawal, F	106.5 MMRB	Eq. 4

EDITOR-IN-CHIEF
Prof. Saeid Eslamian [IRAN]

Results and Discussion

Fluid Classification and Calculated Properties

The fluid is unambiguously classified as a black oil. Over the pressure range of 1,814.7 to 2,689.5 psia, the PVTp tables show a solution gas–oil ratio rising from 371.4 to 579.6 scf/STB, an oil formation volume factor rising from 1.244 to 1.340 RB/STB, an oil viscosity falling from 0.732 to 0.572 cp and an oil density falling from 735.0 to 709.6 kg/m^3 (Table 3). Read in the direction of depletion, these are the changes expected of a solution-gas system: as pressure falls, gas leaves the oil, the oil shrinks by approximately 7%, and its viscosity rises by approximately 28% (Fig. 2). The gas Z-factor changes little, staying between 0.803 and 0.814 with a shallow minimum near 2,300 psia. Water properties vary by less than 3% across the same interval: B_w runs from 1.0291 to 1.0263 RB/STB and the compressibility is approximately 3.08×10^{-6} psi^{-1}. Such near-constant water properties confirm that water expansion is a minor energy source next to aquifer influx.

Table 3. End-Point Fluid Properties from the PVTp Calculation at 195 °F.

Property	At 1,814.7 psia	At 2,689.5 psia	Change on depletion
Solution GOR, R_s (scf/STB)	371.4	579.6	−35.9%
Oil FVF, B_o (RB/STB)	1.244	1.340	−7.2%
Oil viscosity, μ_o (cp)	0.732	0.572	+28.0%
Oil density, ρ_o (kg/m^3)	735.0	709.6	+3.6%
Gas FVF, B_g (ft^3/scf)	0.00832	0.00557	—
Gas density (kg/m^3)	117.7	175.8	—

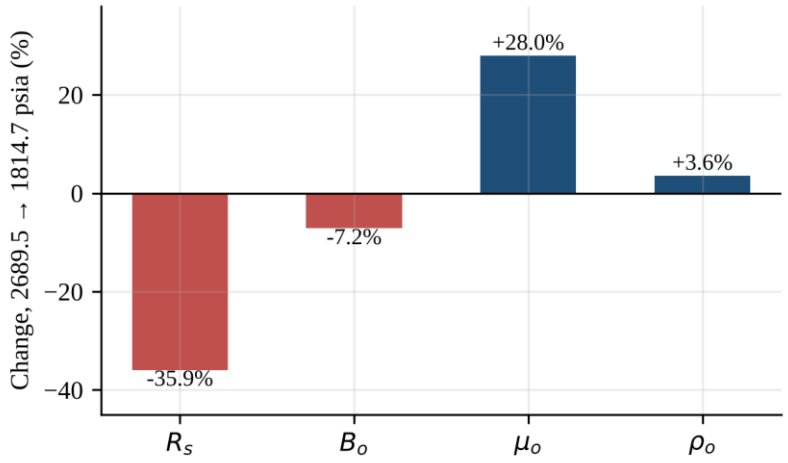

Figure 2: Fractional change of the principal oil properties

Viscosity matters here because it ties the fluid model to well deliverability. Productivity index falls as viscosity rises, so a 28% increase costs deliverability on its own, before any decline in reservoir pressure is counted; the 7% fall in the formation volume factor offsets part of that loss at surface conditions. An error in the fluid model can therefore feed directly into well performance forecasts.

EDITOR-IN-CHIEF
Prof. Saeid Eslamian [IRAN]

Correlation Matching

No single correlation proved best for every property in the regression against laboratory data (Table 4). For bubble point pressure Standing gave the lowest standard deviation (2.44×10^{-8}). Vasquez–Beggs did best for both solution gas–oil ratio (2.726) and oil formation volume factor (0.00283), with Standing a close second on each, and Lasater was the weakest of the six on all three properties. The fitted modifiers stayed close to unity with small shifts, so the fluid is typical of its class and needed only mild tuning. The best correlation is known to change with property and region (Obanijesu et al., 2008; Ikpabi and Akinsete, 2022), which favours choosing correlations property by property instead of adopting one family wholesale.

Table 4. Best and Weakest Correlations by Standard Deviation of the Match.

Property	Best correlation	Std. dev.	Runner-up	Weakest
Bubble point pressure	Standing	2.44×10^{-8}	—	Lasater
Solution GOR	Vasquez–Beggs	2.726	Standing	Lasater
Oil FVF	Vasquez–Beggs	0.00283	Standing	Lasater

One inconsistency needs to be stated. The property tables in Section 3.1 came from the Glaso and Beggs–Robinson selections on the input screen, yet the matching exercise ranked Standing and Vasquez–Beggs highest. Because the PVTp and PROSPER tables are anchored to the laboratory saturation data, the match quality limits the effect on the expansion terms. Even so, the cleaner practice is to regenerate the tables from the best-ranked correlations before the tank model is built, and this appears among the recommendations.

Saturation Pressure and the Initial State

PVTp puts the bubble point at 2,714.7 psia and PROSPER at 2,643.76 psia, where the table is anchored to the measured saturation pressure. At saturation PROSPER returns a solution gas–oil ratio of 566 scf/STB, an oil formation volume factor of 1.3358 RB/STB and a viscosity of 0.579 cp. The 71 psi (2.6%) gap between the two modules is acceptable for engineering work if it is applied consistently, since the saturation pressure marks the change from linear Darcy inflow to the curved, Vogel-type behaviour. What matters more is that the initial pressure of 2,671.7 psia sits within about 43 psi of the PVTp bubble point. Production therefore began essentially at saturation, and the reservoir fell below it almost at once. Free gas was liberated throughout the producing life, and the oil FVF and solution gas terms of Eq. 5 control the expansion energy from the first month of the history.

Pressure and Production History

Between October 2008 and September 2018 cumulative oil production rose from zero to 60.51 MMSTB, while average reservoir pressure dropped from 2,671.7 to 1,726.7 psia, a fall of 945 psi (Fig. 3). The source analysis gives the decline as approximately 930 psi on the psig plot; the 15 psi difference comes from reading the plotted end point against the tabulated value and does not change the conclusions. A decline of 945 psi for 60.5 MMSTB is modest for the volume produced, and on its own it points to an energy source beyond fluid expansion.

EDITOR-IN-CHIEF
Prof. Saeid Eslamian [IRAN]

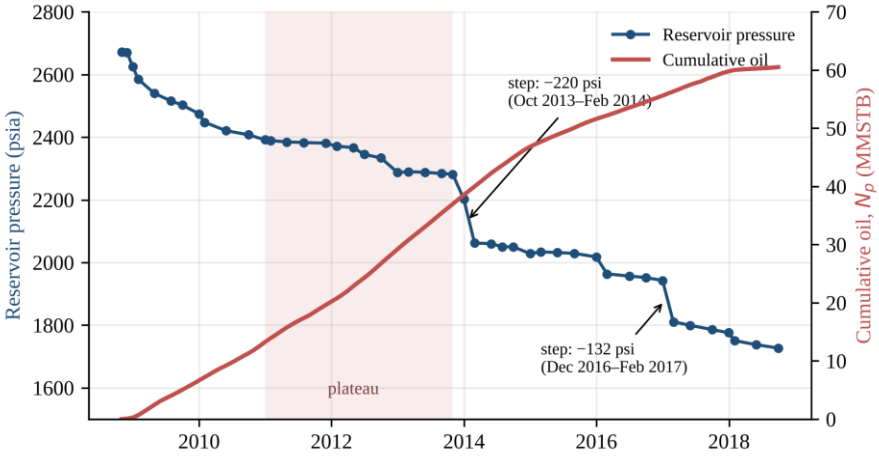

Figure 3. Reservoir pressure and cumulative oil production, October 2008 to September 2018 (replotted from the embedded MBAL history data).

The decline is uneven. The record was split into five phases and a straight line was fitted to pressure against cumulative oil in each (Fig. 4, Table 5). The first phase is a steep initial depletion of 21.4 psi per MMSTB over the first 13 MMSTB. A pronounced plateau follows between 2011 and late 2013, at only 5.7 psi per MMSTB, and after it come discrete drops. The largest, approximately 220 psi, falls between October 2013 and February 2014; a second, approximately 132 psi, falls between December 2016 and February 2017. The source text ties the second drop to 2016, but the tabulated data place it in early 2017. Steps like these in an otherwise smooth record look more like survey-to-survey changes in the pressure data than a physical event, so they are flagged as a data-quality question and not read as aquifer behaviour. The plateau is different. A pressure gradient of 5.7 psi per MMSTB is about a quarter of the initial value, and it fits aquifer support that stayed effective for roughly three years.

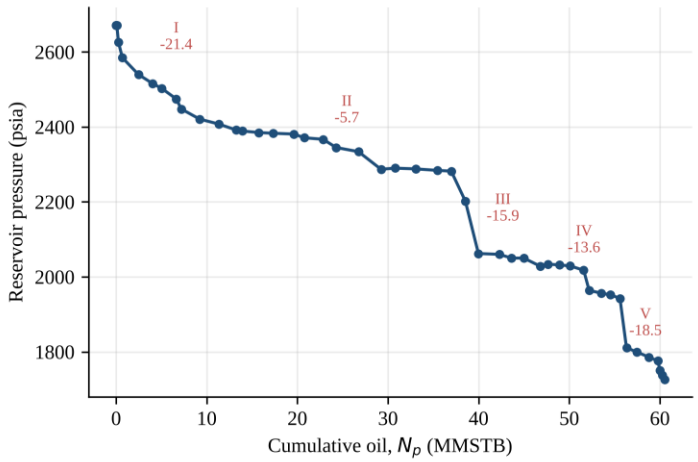

Figure 4: Pressure against cumulative oil production with the five depletion phases

Table 5. Depletion Phases from the History Data (slope of pressure against cumulative oil).

Phase	N_p range (MMSTB)	Pressure (psia)	Slope (psi/MMSTB)	Remark
I	0 – 13.3	2,671.7 → 2,391.7	−21.4	Initial depletion
II	13.9 – 37.0	2,389.0 → 2,282.0	−5.7	Plateau
III	38.5 – 46.8	2,202.0 → 2,028.2	−15.9	After 220 psi step
IV	47.7 – 55.6	2,034.0 → 1,942.5	−13.6	
V	56.3 – 60.5	1,810.7 → 1,726.7	−18.5	After 132 psi step

Aquifer Fitting and Sensitivity

With the Carter–Tracy radial aquifer, the water-drive function fitted by the Fanchi approximation returned $a_0 = 0.96883$, $a_1 = 0.0088745$, $a_2 = 0.213227$ and $a_3 = -0.00602388$ with a standard deviation of 0.1513 (Fig. 5 and Fig. 6a). The history points fell between the dimensionless curves for outer-to-inner radius ratios of about 10 and 15, which supports a large radial aquifer. This configuration returned an oil in place of 500 MMSTB, with a calculated aquifer volume of 1.076×10^6 MMft^3.

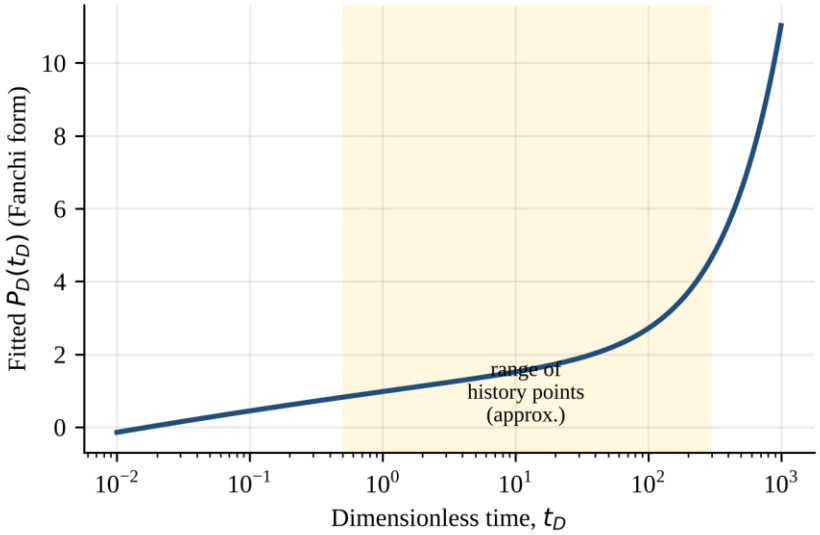

Figure 5: Dimensionless pressure function of Eq. 10, evaluated with the reported coefficients. The shaded band marks roughly the range of dimensionless times spanned by the history points.

The sensitivity analysis showed that the match was controlled mainly by the encroachment angle (Fig. 6b). The standard deviation reached a clear minimum between roughly 120° and 200° and climbed sharply beyond 250°, most severely for the thicker cases; near the minimum, thickness had comparatively little influence. This says something about geometry as well as fit. An angle near 180° corresponds to an aquifer in contact with one flank of the structure, which is more typical of field geometry than a fully encircling aquifer. The initial assumption of 360° was therefore revised, and the Hurst–van Everdingen–Dake model with 180° returned an oil in place of 310 MMSTB (Fig. 6d). The simulated pressure for this configuration reproduced the shape and end point of the history, converging on approximately 1,750 psig by 2018, but it ran 100–150 psi above the observed pressure between 2009 and 2014 and overshot after the 2014 inflection (Fig. 6c). Early aquifer support is

thus slightly overestimated, and the real aquifer response seems somewhat more delayed than the model allows. Forecasts from the present model should accordingly be read as mildly optimistic.

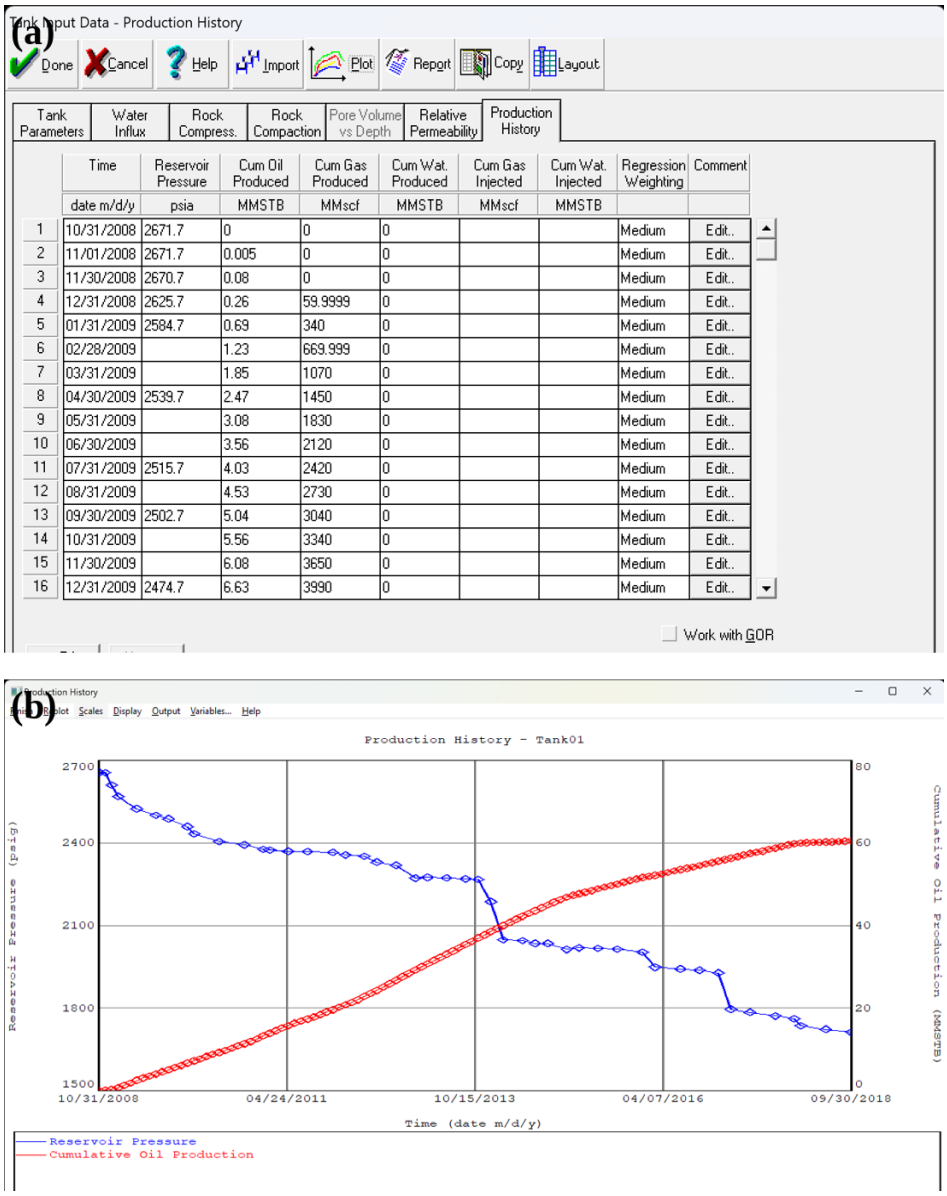

	Time	Reservoir Pressure	Cum Oil Produced	Cum Gas Produced	Cum Wat. Produced	Cum Gas Injected	Cum Wat. Injected	Regression Weighting	Comment
	date m/d/y	psia	MMSTB	MMscf	MMSTB	MMscf	MMSTB		
1	10/31/2008	2671.7	0	0	0			Medium	Edit..
2	11/01/2008	2671.7	0.005	0	0			Medium	Edit..
3	11/30/2008	2670.7	0.08	0	0			Medium	Edit..
4	12/31/2008	2625.7	0.26	59.9999	0			Medium	Edit..
5	01/31/2009	2584.7	0.69	340	0			Medium	Edit..
6	02/28/2009		1.23	669.999	0			Medium	Edit..
7	03/31/2009		1.85	1070	0			Medium	Edit..
8	04/30/2009	2539.7	2.47	1450	0			Medium	Edit..
9	05/31/2009		3.08	1830	0			Medium	Edit..
10	06/30/2009		3.56	2120	0			Medium	Edit..
11	07/31/2009	2515.7	4.03	2420	0			Medium	Edit..
12	08/31/2009		4.53	2730	0			Medium	Edit..
13	09/30/2009	2502.7	5.04	3040	0			Medium	Edit..
14	10/31/2009		5.56	3340	0			Medium	Edit..
15	11/30/2009		6.08	3650	0			Medium	Edit..
16	12/31/2009	2474.7	6.63	3990	0			Medium	Edit..

Figure 6: MBAL aquifer fitting for the initial Carter–Tracy case. (a) Water-drive function match with the Fanchi polynomial coefficients. (b) Sensitivity of the regression standard deviation to encroachment angle (horizontal axis) and reservoir thickness (curves 1–11, 100–200 ft); screen captures from the study software

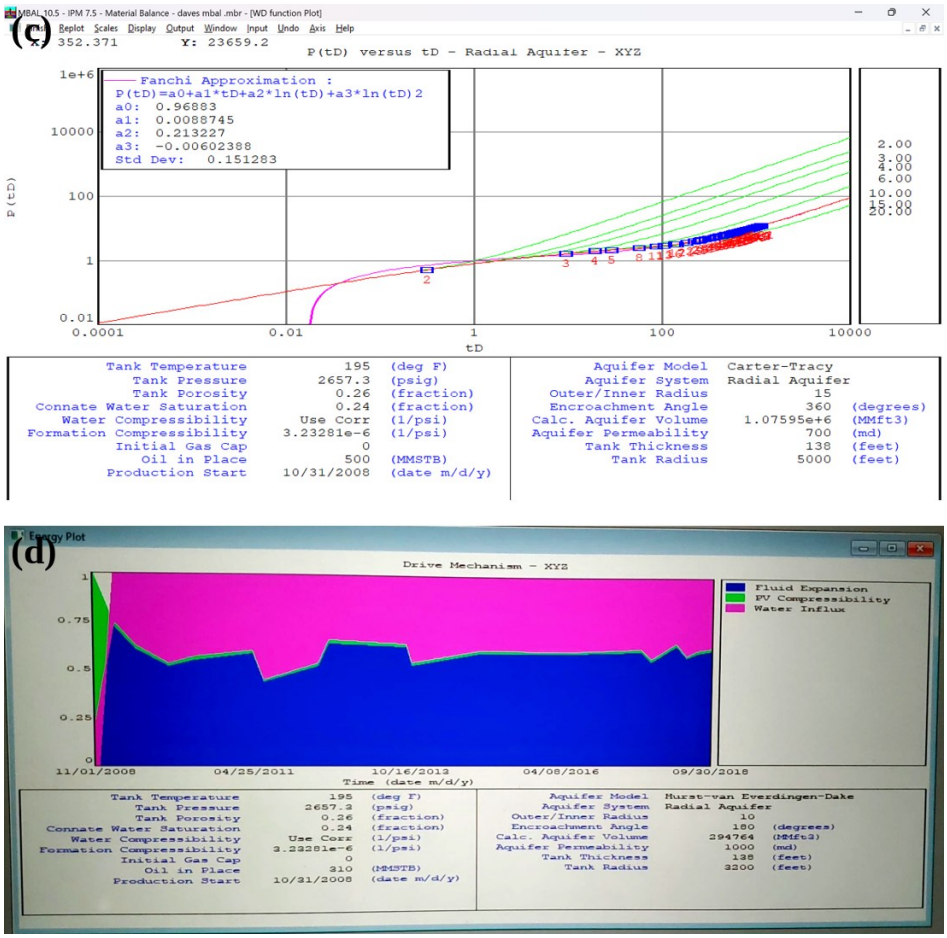

Figure 6: Behaviour of the final model. **(c)** Simulated against historical tank pressure. **(d)** Energy plot for the Hurst–van Everdingen–Dake model, showing fluid expansion (blue), pore-volume compressibility (green) and water influx (magenta); screen captures from the study software.

Oil in Place, Drive Mechanism and Recovery Factor

The oil in place falls from 500 MMSTB under the Carter–Tracy 360° case to 310 MMSTB under the matched Hurst–van Everdingen–Dake 180° case, a difference of 38% (Fig. 7). With the matched value, the 60.51 MMSTB produced to date corresponds to a recovery factor of approximately 19.5% (Eq. 11); under the 500 MMSTB case it would be approximately 12.1%. A recovery factor of that size after ten years of production below the bubble point is plausible for a combination-drive reservoir. It stays well below the 30–60% range quoted for water-drive reservoirs (Al-Mahasneh et al., 2023), which indicates that substantial recoverable oil remains and that the aquifer has not been fully exploited as a displacing agent.

The energy plot shows that fluid expansion and water influx are the two governing mechanisms. After an initial transient dominated by pore-volume compressibility, fluid expansion settles at approximately 55–60% of the total drive energy, water influx supplies the remaining 40–45%, and pore-volume compressibility contributes approximately 2%. The absence of an initial gas cap rules out gas-cap drive. The 38% spread between the two aquifer descriptions is the largest single source

EDITOR-IN-CHIEF
Prof. Saeid Eslamian [IRAN]

of uncertainty in the study, larger than any difference attributable to the fluid correlations, whose modifiers remained close to unity. This is precisely the behaviour that the second argument of this paper anticipates: the fluid description is well constrained by the laboratory data, whereas the aquifer description is constrained only by a pressure history that several aquifers can reproduce.

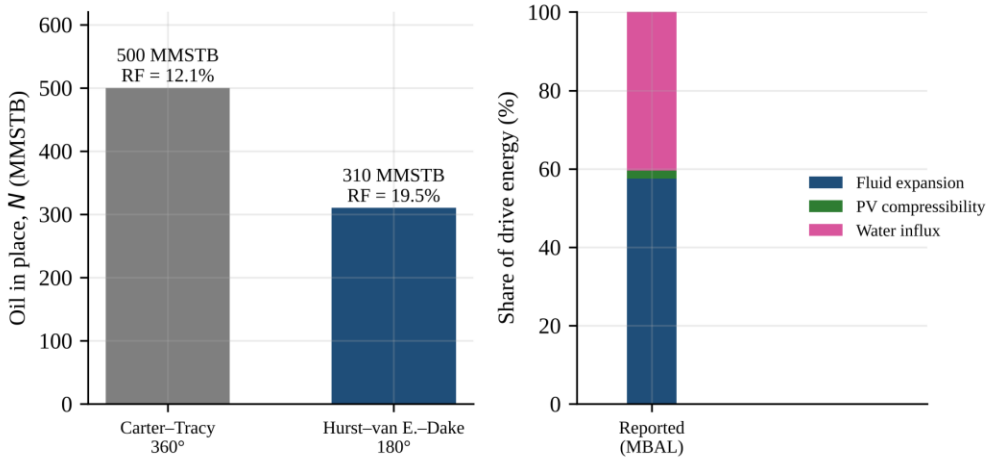

Figure 7: Left: oil in place and recovery factor for the two aquifer configurations. Right: reported partition of drive energy for the matched model (midpoints of the reported ranges)

Independent Energy-Budget Check

The energy-budget check gives an underground withdrawal F of 106.5 MMRB at the end of the history for R_p = 700 scf/STB, and 101.9 and 111.1 MMRB for the lower and upper brackets. The oil expansion term E_o is 0.2197 RB/STB and the rock-and-water term $E_{f,w}$ is 0.0064 RB/STB. For the matched value N = 310 MMSTB, expansion of oil, dissolved gas, rock and water accounts for approximately 70 MMRB, or 63–69% of F across the bracket, which leaves an implied water influx of approximately 36 MMRB (range 32–41 MMRB) (Fig. 8, Table 6). This expansion share is somewhat above the 55–60% shown by the regression. That is expected: the check uses an endpoint value with extrapolated properties, whereas the regression follows the share through time. The two are of the same order and point the same way. At N = 500 MMSTB the picture changes. The expansion terms alone, approximately 113 MMRB, exceed the underground withdrawal in every case of the bracket, and the implied water influx is negative, between −2 and −11 MMRB, which is physically inadmissible.

Table 6. Energy-budget check at the end of the history (60.51 MMSTB produced).

Quantity	R_p = 650	R_p = 700	R_p = 750
Withdrawal, F (MMRB)	101.9	106.5	111.1
N_{max} at W_e = 0 (MMSTB)	451	471	491
Implied W_e for N = 310 (MMRB)	31.8	36.4	41.0
Expansion share for N = 310 (%)	68.8	65.8	63.1
Implied W_e for N = 500 (MMRB)	−11.2	−6.6	−2.0

EDITOR-IN-CHIEF
Prof. Saeid Eslamian [IRAN]

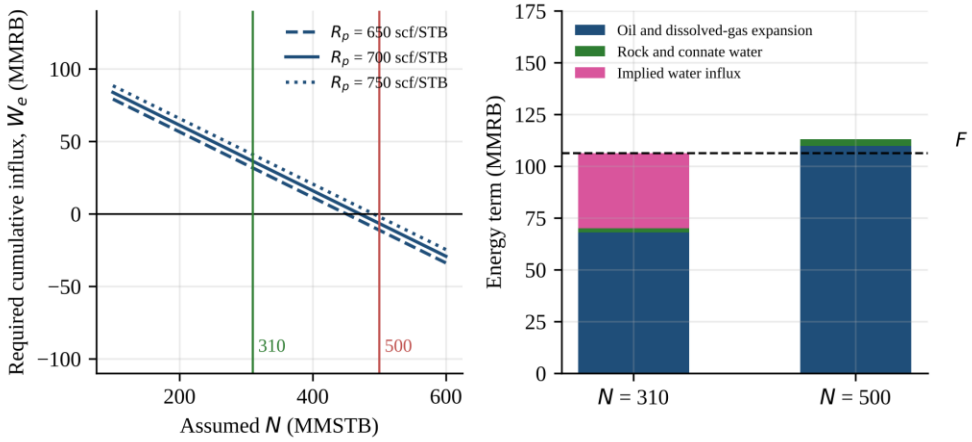

Figure 8: Independent Havlena–Odeh check. Left: water influx required to balance the withdrawal as a function of assumed oil in place, for three produced gas–oil ratios. Right: energy budget for the two oil-in-place values at R_p = 700 scf/STB.

Two inferences follow. First, the energy balance caps the oil in place at approximately 450–490 MMSTB over the plausible range of R_p. The 360° Carter–Tracy result of 500 MMSTB therefore lies outside the admissible range under the stated assumptions, and the 180° result of 310 MMSTB lies comfortably inside it. Second, the check does not prove 310 MMSTB. It sets an upper bound only, and any value between zero and approximately 470 MMSTB satisfies it for some influx, so an independent volumetric or well-test constraint is still needed. The result also depends on the initial formation volume factor. Using the PVTp value of approximately 1.340 RB/STB in place of the laboratory 1.3358 RB/STB lowers E_o by about 2% and raises the bound to approximately 460–500 MMSTB. At the upper end of the R_p bracket the 500 MMSTB case would then be admissible only with zero water influx, which would contradict the aquifer support evident in the pressure plateau. The practical value of the check is that a few lines of arithmetic screen out inadmissible aquifer models before the more expensive volumetric or simulation work starts, a use consistent with the integrated, multi-method approach recommended by Fuentes-Cruz et al. (2021).

Ranking the Sources of Uncertainty

The analysis allows the sources of uncertainty to be compared on a common footing, namely their effect on the estimate of oil in place or on the energy terms from which it is derived (Table 7). The aquifer description dominates by a wide margin: changing from the 360° Carter–Tracy to the 180° Hurst–van Everdingen–Dake configuration alters the oil in place by 190 MMSTB, or 38% of the larger value. By contrast, the bracket on the produced gas–oil ratio alters the underground withdrawal by approximately ±4%, the choice of initial formation volume factor alters the oil expansion term by approximately 2%, and the correlation modifiers, which stay close to unity, imply that the fluid description is constrained to within a few per cent by the laboratory data. The ranking is not an accident of this field. It follows from the structure of Eq. 6, in which the fluid properties multiply the oil in place directly through E_o whereas the aquifer enters as an additive term whose magnitude

is, in the absence of independent data, free to absorb whatever the pressure history leaves unexplained.

Table 7. Sources of uncertainty ranked by effect on the results.

Source	Quantified effect	Basis
Aquifer model and angle	190 MMSTB (38%) on oil in place	MBAL regressions, 500 vs 310 MMSTB
Aquifer parameters (thickness)	Small near the minimum of the sensitivity surface	Sensitivity analysis, 100–200 ft
Produced GOR, R_p	approx. ±4% on F; 451–491 MMSTB on N_{max}	Energy-budget check
Initial FVF, B_{oi}	approx. 2% on E_o	Energy-budget check
Correlation choice	Modifiers near unity; best-fit σ small	PVTp match
Pressure data steps	220 and 132 psi discrete drops	History data

Comparison with Published Work

The findings are consistent with the wider literature in three respects. First, the preference for different correlations for different properties echoes regional evidence that imported correlations do not transfer uniformly to Niger Delta crudes, where locally derived models and machine-learning approaches have outperformed them for bubble-point pressure and formation volume factor (Ikpabi and Akinsete, 2022). The present result differs only in that the global correlations Standing and Vasquez–Beggs, after mild regression, reproduced the laboratory data for this fluid well, suggesting that a regression-tuned global correlation is an adequate substitute when a regional model is not available. Second, the sensitivity of the oil in place to the aquifer model agrees with MBAL case studies in which the choice among influx models changed the quality of the regression and the inferred aquifer size (Nmegbu et al., 2021; Saleh et al., 2025), and with the general warning that a good history match does not guarantee a correct reservoir–aquifer model (Fuentes-Cruz et al., 2021). Third, a strong aquifer inferred from a modest pressure decline matches interpretations of water-drive reservoirs elsewhere, where early or sustained pressure support is often the first sign of influx (Al-Mahasneh et al., 2023; Aliu et al., 2024).

This study adds a transparent link between these strands. The energy-budget check converts the qualitative warning about non-uniqueness into a quantitative screen. It shows which of the two competing aquifer models is energetically admissible, needs no additional data, and uses only quantities the engineer already has. Its limitation is just as plain: the check caps the oil in place but cannot fix it, and a volumetric estimate, which the present data set does not provide, remains the natural complement.

Integrated Implications

The three stages share a single fluid description, and it runs through the whole analysis. A bubble point marginally below the initial pressure makes the reservoir a depletion-and-influx system from its first month. Rising viscosity governs how quickly deliverability decays, and the falling formation volume factor sets how many reservoir barrels are needed per stock-tank barrel. The aquifer

EDITOR-IN-CHIEF
Prof. Saeid Eslamian [IRAN]

supplies 40–45 % of the energy; it explains the Phase II plateau and the modest overall pressure decline that has let the reservoir produce at moderate pressure for a decade. The expansion terms are built from the PVT table, so any error in the fluid model passes into the aquifer fit and then into the oil in place. The fluid and aquifer descriptions are therefore not independent, even though their individual uncertainties differ in size.

Field management follows from these findings. The reservoir began production at its bubble point, has a recovery factor of approximately 19.5 % after ten years, and its aquifer-supported pressure plateau is now giving way to steeper decline. Two decisions matter most from here. The first is surveillance. The pressure record contains discrete steps of 220 and 132 psi that cannot be diagnosed without more frequent and better-documented measurements, and a more regular programme would allow the aquifer response to be tracked rather than inferred. The second is well performance. Viscosity rises by approximately 28 % between the bubble point and 1,814.7 psia while the formation volume factor falls by 7 %, so the inflow performance relationship of each well will shift downward and toward the curved form as average pressure declines below saturation. Nodal analysis in PROSPER, fed with the PVTp table used here, is the natural next step for testing whether artificial lift or pressure maintenance would be needed to hold the production plateau. The fluid model of this study is thus a common foundation for reservoir and well calculations, not an end product, which is why it is kept consistent across modules.

Several limitations bound these conclusions. The reservoir is represented as a single tank, so areal and vertical heterogeneity, saturation distribution and compartmentalisation are averaged out. The material-balance solution is non-unique, as the 38 % spread shows, and independent volumetric or well-test data are needed to choose among the remaining admissible values. Gas viscosity is reported as zero in the PVTp output, which indicates that it was not computed; it must be populated before the model is used for gas-dominated calculations. The history match runs 100–150 psi optimistic through the middle of the record. The independent check is first-order and rests on an assumed produced gas–oil ratio and extrapolated properties.

Conclusions

1. Reservoir XYZ is a black oil (35 °API, 700 scf/STB produced GOR). Over 2,689.5–1,814.7 psia, Rs falls from 579.6 to 371.4 scf/STB (−35.9 %), Bo falls from 1.340 to 1.244 RB/STB (−7.2 %), μo rises from 0.572 to 0.732 cp (+28.0 %) and ρo rises by 3.6 %. The gas Z-factor is near-constant (0.803–0.814) and water properties vary by less than 3 %, confirming that water expansion is a minor energy source.
2. The initial pressure (2,671.7 psia) sits within about 43 psi of the PVTp bubble point. Production therefore began essentially at saturation and the reservoir went below bubble point almost at once.
3. No single correlation was best for all properties: Standing for Pb ($\sigma = 2.44 \times 10^{-8}$), Vasquez–Beggs for Rs ($\sigma = 2.726$) and Bo ($\sigma = 0.00283$), with Standing a close runner-up and Lasater weakest throughout. Fitted modifiers stayed close to unity.
4. Production of 60.51 MMSTB was accompanied by a 945 psi pressure decline that is non-uniform: steep initial depletion (21.4 psi/MMSTB), a pronounced plateau (5.7 psi/MMSTB, 2011–late 2013), and discrete steps of ≈ 220 psi and ≈ 132 psi. The steps are treated primarily

EDITOR-IN-CHIEF
Prof. Saeid Eslamian [IRAN]

as data-quality issues that may also reflect gauge recalibration, incomplete shut-in stabilisation or local compartmentalisation; the plateau is consistent with effective aquifer support for roughly three years.

5. The Carter–Tracy 360° case returned 500 MMSTB. Sensitivity analysis showed the match to be controlled mainly by encroachment angle, with a standard-deviation minimum between roughly 120° and 200°. The revised 180° Hurst–van Everdingen–Dake model returned 310 MMSTB—a 38 % difference and the largest single uncertainty in the study. The final model runs 100–150 psi above observed pressure through 2009–2014 and should be regarded as mildly optimistic.
6. Fluid expansion supplies ≈ 55–60 % of drive energy, water influx 40–45 % and pore-volume compressibility ≈ 2 %, with no gas-cap drive. Recovery factor is ≈ 19.5 % at 310 MMSTB versus ≈ 12.1 % at 500 MMSTB.
7. The independent energy budget (F = 106.5 MMRB at Rp = 700 scf/STB) implies ≈ 36 MMRB of water influx for N = 310 MMSTB. At N = 500 MMSTB expansion alone exceeds withdrawal and the implied influx is negative (−2 to −11 MMRB), which is inadmissible. The check therefore caps OOIP at ≈ 450–490 MMSTB without fixing its exact value.
8. Uncertainty ranking places the aquifer model and angle (190 MMSTB, 38 %) well ahead of produced GOR (±4 % on F), initial FVF (≈ 2 % on Eo), correlation choice (modifiers near unity) and the pressure-data steps.

Recommendations

1. Constrain OOIP independently by a volumetric estimate and by well-test data, because material balance alone cannot separate the admissible aquifer descriptions.
2. Regenerate the PVTp tables from the best-ranked correlations (Standing for Pb; Vasquez–Beggs for Rs and Bo) and populate gas viscosity before refining the tank model.
3. Maintain pressure surveillance at a frequency sufficient to resolve the 220 psi and 132 psi step changes, since the aquifer supplies nearly half of the drive energy.
4. Evaluate pressure maintenance by water injection, given the ≈ 19.5 % recovery factor, continuing decline and viscosity-driven deliverability loss.
5. Extend the work to a probabilistic analysis that jointly samples aquifer parameters and fluid correlations, and to three-dimensional simulation that captures the heterogeneity averaged out by the single-tank representation.
6. Carry the consistent PVT table into PROSPER for nodal analysis to test artificial-lift or pressure-maintenance options as inflow shifts toward Vogel-type behaviour below saturation.

References

Ahmed, T. (2019). *Reservoir Engineering Handbook* (5th ed.). Gulf Professional Publishing.

Alatefi, S., & Almeshal, A. M. (2021). A New Model for Estimation of Bubble Point Pressure Using a Bayesian Optimized Least Square Gradient Boosting Ensemble. *Energies, 14*(9), 2653. https://doi.org/10.3390/en14092653

Aliu, H. O., Alawode, A. J., & Falade, A. A. (2024). Material balance analysis of water influx into an undersaturated oil reservoir using pot aquifer model: A case study. Geosystem Engineering, 28(1), 46–60. https://doi.org/10.1080/12269328.2024.2417076

EDITOR-IN-CHIEF
Prof. Saeid Eslamian [IRAN]

Al-Mahasneh, M., Al-Khasawneh, H. E., Al-Zboon, K., Al-Mahasneh, M., & Aljarrah, A. (2023). Water Influx Impact on Oil Production in Hamzeh Oil Reservoir in Northeastern Jordan: Case Study. *Energies, 16*(5), 2126. https://doi.org/10.3390/en16052126

Fotias, S. P., Georgakopoulos, A., & Gaganis, V. (2022). Workflows to Optimally Select Undersaturated Oil Viscosity Correlations for Reservoir Flow Simulations. *Energies, 15*(24), 9320. https://doi.org/10.3390/en15249320

Fuentes-Cruz, G., & Vásquez-Cruz, M. A. (2022). Reservoir performance analysis through the material balance equation: An integrated review based on field examples. *Journal of Petroleum Science and Engineering, 208*, 109377. https://doi.org/10.1016/j.petrol.2021.109377

Jongkittinarukorn, K., & Kabir, C. S. (2023). A novel material-balance approach for estimating in-place volumes of gas and water in gas reservoirs with aquifer support. *Journal of Petroleum Exploration and Production Technology, 13*, 1627–1640. https://doi.org/10.1007/s13202-023-01630-5

Ikpabi, P. B., & Akinsete, O. O. (2022). Correlation for predicting bubble point pressure for 22.3≤°API≥45 crude oils: A white-box machine learning approach. International Journal of Frontiers in Engineering and Technology Research, 3(2), 15–27. https://doi.org/10.53294/ijfetr.2022.3.2.0043

Li, Y., Li, B., & Yu, W. (2024). A Novel Method to Calculate Water Influx Parameters and Geologic Reserves for Fractured-Vuggy Reservoirs with Bottom/Edge Water. *Energies, 17*, 2822. https://doi.org/10.3390/en17122822

Li, Y., Li, B., & Yu, W. (2025). Material Balance Equation for Fractured Vuggy Reservoirs with Aquifer Multiples: Case Study of Fuman Oilfield. *Energies, 18*, 3550. https://doi.org/10.3390/en18133550

Nmegbu, G. C., & Wachukwu, M. E. (2021). Reservoir Fluids Estimation and Modelling using MBAL for a Case Study of a Typical Limestone Formation. *International Journal of Engineering Research and Applications, 11*, 26–64.

Obanijesu, E. O., et al. (2008). Development of a correlation for predicting the formation volume factor of Nigerian crude oils. Journal of Petroleum Science and Engineering.

Papanikolaou, P., Kanakaki, E. M., Lempesis, S., & Gaganis, V. (2024). Mass Balance-Based Quality Control of PVT Results of Reservoir Oil DL Studies. *Energies, 17*, 3301. https://doi.org/10.3390/en17133301.

Saleh, L. D., Alhaj, H. K., Traki, A. R., Alshebany, A. A., Barammith, M. R., & Marghani, M. M. (2025). Modeling of an oil reservoir in Field "X" to understand its behavior with emphasis on the effect of water influx. *International Science and Technology Journal*. https://doi.org/10.62341/moxi1016

Tian, Y., Li, B., & Yu, W. (2025). New Method for Calculating Rock Compressibility, Dynamic Reserves, and Aquifer Size for Fractured–Vuggy Reservoirs with Bottom Aquifer. *Processes, 13*, 684. https://doi.org/10.3390/pr13030684

Yao, C., Yan, R., Zhou, F., Zhang, Q., Niu, G., Chen, F., Cao, W., & Wang, J. (2024). A Novel Method to Calculate Water Influx Parameters and Geologic Reserves for Fractured-Vuggy Reservoirs with Bottom/Edge Water. *Energies, 17*, 2822. https://doi.org/10.3390/en17122822

EDITOR-IN-CHIEF
Prof. Saeid Eslamian [IRAN]